Journal of Functional Materials and Applied Engineering

Research Paper

Preparation and Properties of Cellulose Nanocrystal-Based Structurally Colored Radiative Cooling Composite Films

Ali Okonkwo [1], Matthew Ayyash [1], Malli Comer [2,*], Raivis Izaks [2]

[1] Institute of Forest Science, CSIC, Ctra. de la Coruña, km 7,5, Madrid 28040, Spain
[2] Laboratory of Advanced Materials and Devices, Department of Physics, Aristotle University of Thessaloniki, 54124, Thessaloniki, Greece

*Corresponding author: Malli.comer@physics.auth.gr

Abstract. Radiative cooling lowers its own temperature by emitting heat into outer space, is a green, low-carbon, and sustainable cooling strategy. Most radiative cooling materials have monotonous appearance colors, mostly white or transparent, and the addition of traditional colorants will cause the materials to absorb heat, reducing radiative cooling performance. Structurally colored cellulose nanocrystal/polyethylene glycol (CNC/PEG) composite radiative cooling films were prepared by self-assembly method, and the composite films were combined with porous cellulose acetate (CA) membranes to obtain structurally colored radiative cooling bilayer composite films. The results show that the CNC/PEG composite films have bright structural colors with obvious birefringence phenomenon. As the PEG content increases, the pitch of the composite film structure increases, and the color changes from blue-green to red. The CNC/PEG structurally colored composite film has the highest reflectance in the visible light band up to 68.5%, and the emissivity in the atmospheric window band is up to 93%, with an ambient cooling effect of about 3.4°C. The CNC/PEG-CA bilayer composite film has the highest reflectance in the visible light band up to 91.8%, and the emissivity in the atmospheric window band is up to 32.2%. Compared with the composite film, the bilayer composite film has better cooling performance, with a temperature difference of about 14.3°C compared to the ambient temperature. In outdoor tests, compared with the ambient temperature, the composite film can achieve a cooling effect of about 2°C, and the bilayer composite film can achieve a cooling effect of about 6°C.

Keywords: *Radiative cooling; Structural color; Cellulose nanocrystals; Chiral nematic structure; Bilayer composite film*

Received on 15 Sep 2024, Accepted on 15 Oct 2024, Published on 15 Dec 2024

1 Introduction

Currently, the negative effects of global warming greatly affect human production and life [1-2]. Excessive energy consumption and scarcity further increase environmental problems, how to do thermal management is the main problem currently faced [3-5]. The Earth's surface temperature is 300K, while the average temperature of outer space is 3K [6-7]. In accordance with the second law of thermodynamics, thermal energy from terrestrial bodies may be dissipated to the cosmic void through electromagnetic radiation driven by temperature gradients. Consequently, radiative cooling technology exploits this principle by enabling surface materials to emit infrared radiation predominantly through the atmospheric transmission window (8–13 μm) [8–10], thereby attaining passive temperature reduction without external energy input.

Although radiative cooling materials show great application potential in energy saving and environmental protection [10], existing materials are mostly white or silver-white, with monotonous appearance and low utilization rate. Dyes will change the surface color of materials, but the visible color of dyes will absorb heat and absorb additional heat in the near-infrared band [11-12], reducing the cooling effect of the material itself. So far, the main strategy to overcome this problem is to improve the reflectance in the visible region and the emissivity in the "atmospheric window" band (8~13 μm) [13-16]. To avoid the phenomenon of dye heat absorption, structurally colored radiative cooling materials have attracted widespread attention. Using silicon opals can

prepare radiative cooling materials with structural color changes, but this method cannot achieve sub-ambient cooling [19], and the production process and conditions are complex and harsh, making it difficult for large-scale production and application.

Cellulose nanocrystals constitute stiff, elongated rod-like nanostructures exhibiting longitudinal dimensions spanning tens to hundreds of nanometers and transverse diameters approaching several tens of nanometers [20], distinguished by elevated crystalline order and favorable environmental degradability. These nanoscale entities may be isolated from replenishable lignocellulosic feedstocks including cotton fibers, woody biomass, and processed pulp, offering advantageous attributes of economic accessibility, ecological compatibility, and renewable sourcing [21–23]. Upon dispersion in aqueous media, cellulose nanocrystals undergo self-assembly into a lyotropic cholesteric mesophase characterized by helicoidal molecular ordering. This organized supramolecular architecture persists throughout solvent evaporation, ultimately yielding solid-state films retaining the chiral nematic organization [24]. The periodic helical stacking of optically anisotropic nanorods within the dried matrix generates spatially modulated refractive index variations, producing intense constructive interference of visible wavelengths [25]. Consequently, the tunability of resultant structural coloration is intimately coupled to the pitch length of the helicoidal superstructure.

Current research is dedicated to manufacturing cellulose radiative cooling materials with richer colors. Shanker et al. [26] obtained a structurally colored radiative cooling device by combining self-assembled CNC structurally colored films with silicon wafer substrates. By controlling the mass ratio of CNC/glycerol (GLU), composite films with colors changing from blue-violet to red were obtained. The structurally colored composite films exhibited low absorption in the solar spectrum range and high emissivity in the "atmospheric window", and the cooling effect of green and red samples could reach about 9°C, while the cooling effect of blue-violet samples could reach about 6°C, providing a research basis for the preparation of cellulose structurally colored radiative cooling films.

This investigation employs a co-assembly strategy integrating cellulose nanocrystals with polyethylene glycol to fabricate photonic films exhibiting elevated solar reflectance coupled with selective thermal emittance within the atmospheric transmission window. Modulation of the carbohydrate-to-polyether mass ratio enables precise tuning of the resultant structural hue, thereby facilitating band-specific regulation of radiative heat dissipation. The influence of varying polyether loading on the morphological features, optical response characteristics, and passive cooling efficacy of the nanocrystal-based photonic composites is systematically examined. Furthermore, these structurally colored layers are laminated onto cellulose acetate microporous substrates to construct dual-layer architectures, with subsequent evaluation of their radiative cooling performance.

2 Materials and Methods

2.1 Experimental Process

Isolation of Cellulose Nanocrystals: The nanoscale cellulosic entities were extracted through controlled acid-catalyzed depolymerization. Specifically, 200 mL of aqueous sulfuric acid (64% v/v) was carefully introduced to 25 g of foliar biomass pulp with continuous mechanical agitation, followed by thermal treatment in a thermostated water bath at 45°C. Hydrolytic cleavage was terminated through substantial dilution with distilled water. The resulting dispersion was permitted to undergo gravitational phase separation, with the supernatant subsequently subjected to repeated purification cycles involving aqueous resuspension and high-speed centrifugal sedimentation (Shanghai Tianmei Instrument Co., Ltd.). The purified colloidal suspension was then transferred to semipermeable membranes for exhaustive dialysis against deionized water until neutral pH was attained. The final nanocrystal dispersion was concentrated to 3% solids content and maintained under refrigerated storage for subsequent utilization.

Fabrication of Nanocrystal-Polyether Hybrid Films: A quantity of 5.0 g polyethylene glycol was dissolved in 45 g ultrapure water under ambient temperature agitation for sixty minutes to yield a 10% polymer stock solution. Aliquots of the 3% nanocrystal dispersion were subjected to five-minute ultrasonic homogenization prior to formulation. Four separate 3.0 g portions of the treated nanocrystal suspension were then blended with 0.1000

g, 0.2250 g, 0.3857 g, and 0.6000 g of the polyether solution respectively. Each formulation underwent thorough mixing for two hours before transfer to circular casting vessels. Controlled evaporation under ambient conditions over 48–72 hours yielded photonic composite films with final polymer loadings of 10%, 20%, 30%, and 40% by mass. The resulting specimens were designated CNC/PEG-10%, CNC/PEG-20%, CNC/PEG-30%, and CNC/PEG-40% according to compositional parameters detailed in Table 1.

Table 1 Naming of Cellulose Nanocrystal/Polyethylene Glycol (CNC/PEG) Composite Radiative Cooling Films and CNC/PEG-Cellulose Acetate (CA) Structurally Colored Radiative Cooling Bilayer Composite Films

Sample	Mass fraction of CNC/wt%	Mass fraction of PEG/wt%	Mass of CA
CNC/PEG-10%	3	10	—
CNC/PEG-20%	3	20	—
CNC/PEG-30%	3	30	—
CNC/PEG-40%	3	40	—
CNC/PEG-10%-CA	3	10	0.0740 g
CNC/PEG-20%-CA	3	20	0.0740 g
CNC/PEG-30%-CA	3	30	0.0740 g
CNC/PEG-40%-CA	3	40	0.0740 g

Preparation of Bilayer Composite Films: Different mass ratio composite structurally colored films and cellulose acetate films are stuck together with double-sided tape, the double-sided tape is placed on the edge of the cellulose acetate film for fixation, will not affect the structure of the bilayer composite structurally colored films, the bilayer composite structurally colored films are named CNC/PEG-10%-CA, CNC/PEG-20%-CA, CNC/PEG-30%-CA, details see Table 1.

2.2 Testing and Characterization

2.2.1 Performance Analysis of CNC/PEG Composite Films

The electrokinetic potential and hydrodynamic dimensions of the nanocrystalline cellulose were determined employing a Malvern Zetasizer Nano ZS90 instrument. The mesomorphic characteristics of the composite specimens were examined through polarized optical microscopy (XPF-550C, Shanghai Caikang Optical Instrument Company). The specular reflectance properties of the prepared films across the visible electromagnetic spectrum were quantified utilizing a high-resolution fiber-optic spectrometer (HR4000 CG-NIR, Ocean Optics). The composite specimens were fractured under cryogenic conditions using liquid nitrogen, subsequently mounted onto aluminum stubs utilizing electrically conductive double-sided tape, and subjected to sixty-second sputter deposition of gold to ensure surface conductivity. The resulting cross-sectional architectures were then examined employing a field-emission scanning electron microscope (JSM-7500F, JEOL Ltd., Japan). Diffuse reflectance spectra (300–2500 nm) were recorded on a PerkinElmer UV-VIS-NIR spectrophotometer equipped with an integrating sphere; mid-IR absorption (2.5–25 μm) was measured on a Thermo Nicolet IS10 FTIR spectrometer. A solar-simulator (Zhongjiao Jinyuan HXF300, Xe arc) served as the light source. A 1 cm^3 cavity was cut in a polystyrene foam box; the film specimen was mounted in the aperture, and the assembly was sealed with polyethylene film to suppress convective heat losses. A multi-channel thermometer (JINKO JK804) with two K-type thermocouples recorded cavity temperature beneath the film and ambient temperature inside the polyethylene enclosure, respectively. Since the CNC/PEG-40% composite film will absorb environmental moisture during characterization, the chiral structure swells, and the pitch changes in actual measurement, which is not conducive to the practical application of the composite film in the actual environment, therefore, subsequent scanning electron microscopy, spectroscopy, and radiative cooling performance testing and analysis will not be performed on the CNC/PEG-40% composite film.

2.2.2 Performance Analysis of Bilayer Composite Films

Cellulose acetate films were adhered to a horizontal stage with conductive tape, sputter-coated with Au for 60 s, and imaged by SEM. Under identical Xe-lamp illumination, surface temperature evolution was monitored with a FLIR E390 infrared camera. The custom-built apparatus recorded both the sub-film cavity temperature and the bulk ambient temperature within the polyethylene-sealed enclosure. Use a laboratory self-assembled device to

DOI:

test the outdoor cooling performance of samples, place the indoor self-assembled cooling performance testing device in a cardboard box wrapped with aluminum foil, place the whole on a foam box, record the ambient humidity changes during the test with a hygrometer.

3 Results and Discussion

3.1 Potential Particle Size Analysis of Cellulose Nanocrystals

Figure 1 shows the TEM image, particle size distribution, and potential curve of CNC. CNC prepared by acid hydrolysis has a rod-like morphology, with an average particle size of 144.1 nm (Fig. 1(b)). During hydrolysis, the CNC surface forms more negative charges, with a Zeta potential as high as -32.2 mV (Fig. 1(c)). The more negative charges on the CNC surface will promote electrostatic repulsion, enhancing the stability of the CNC solution, laying the foundation for the further preparation of structurally colored composite films.

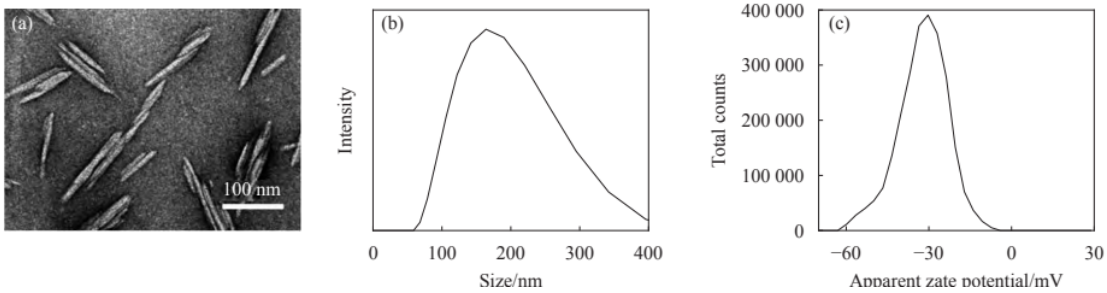

Figure 1 a) TEM image of CNC; (b) Particle size distribution of CNC; (c) Potential curve of CNC

3.2 Analysis of Structural Color Optical Characteristics of Cellulose Nanocrystal Composite Films

Figures 2a–d show that raising PEG content progressively red-shifts the structural colour of the composite films from blue-green toward red, confirming that PEG loading tunes the photonic band gap. UV–vis reflectance (Fig. 2e) places the reflection maxima at 427, 487, 576 and 654 nm for the four PEG loadings, respectively, quantifying the red shift seen by eye. Through Fig. 2(f), it can be known that the composite film achieves self-cooling by reflecting visible light and emitting heat, providing a theoretical basis for subsequent radiative cooling research.

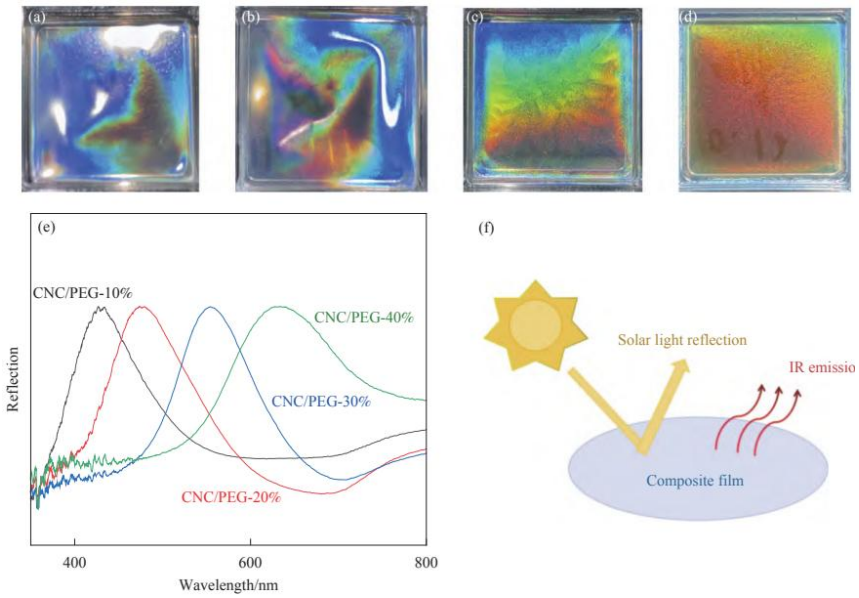

Figure 2 ((a)-(d)) Digital photographs of CNC/PEG-10%, CNC/PEG-20%, CNC/PEG-30%, CNC/PEG-40%; (e) UV-vis reflection spectra of CNC/PEG; (f) Composite film radiative cooling schematic

3.3 Microstructure Analysis of Cellulose Nanocrystal Composite Films

Figures 3(a) to 3(c) are scanning electron microscopy images of the cross-sections of composite films with different PEG contents. When the PEG content is 40%, the composite film will absorb moisture from the environment, the chiral structure swells, and the pitch changes in actual measurement, therefore, only composite films with PEG content of 10% to 30% are studied by scanning electron microscopy, and CNC/PEG-40% composite film is not tested and analyzed by scanning electron microscopy. Neat CNC self-assembles into a left-handed chiral nematic helix that Bragg-reflects left-circularly polarised light of a specific wavelength, conferring iridescent structural colour on the film. Polymer addition preserves the CNC chiral nematic order; however, increasing polymer content enlarges the helical pitch P—the distance over which CNC rods rotate 360°, visible as the inter-layer spacing in SEM.

The reflected light of the CNC/PEG composite film follows the Bragg equation:

$$\lambda = nP\cos(\theta) \qquad (1)$$

Where λ is the reflected wavelength, n the mean refractive index, θ the incidence angle and P the helical pitch. Because CNC (n ≈ 1.41) and PEG (n ≈ 1.44) are optically matched, n remains essentially constant; at fixed θ, λ scales directly with P. The average pitches in Figs. 3(a) to 3(c) are 0.30, 0.36, and 0.46 μm, respectively. As the average pitch P increases, the reflected wavelength λ also gradually increases, the main reason is that after adding PEG, the PEG polymer enters the CNC chiral nematic structure, causing the pitch P of the CNC chiral nematic structure to increase, and the composite film color shifts red.

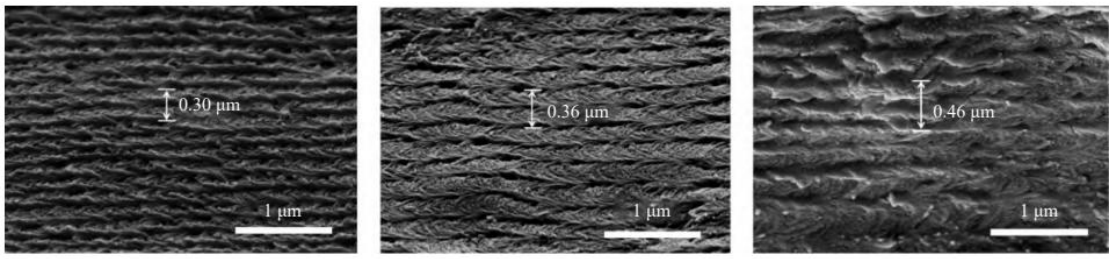

Figure 3 Cross-sectional electron microscope images of composite films with different PEG contents

3.4 Refraction Phenomenon of Cellulose Nanocrystal Composite Films

Polarised-light micrographs (Fig. 4a–d) reveal strong birefringence; high-magnification views (Fig. 4e–h) display characteristic fingerprint textures, confirming that CNC/PEG spontaneously adopts a chiral nematic order during drying and that this helix survives in the solid film. Moderate PEG loading therefore leaves the CNC chiral nematic architecture intact. The fingerprint periodicity widens progressively—2.05, 2.33, 2.84 and 3.38 μm—matching the visual shift from blue-green toward blue-red. PEG intercalates between CNC rods in the helix, expanding the pitch P and red-shifting the reflected colour. POM thus confirms that PEG preserves both the chiral nematic order and birefringence, while offering a convenient handle—PEG content—to tune layer spacing and hence structural hue.

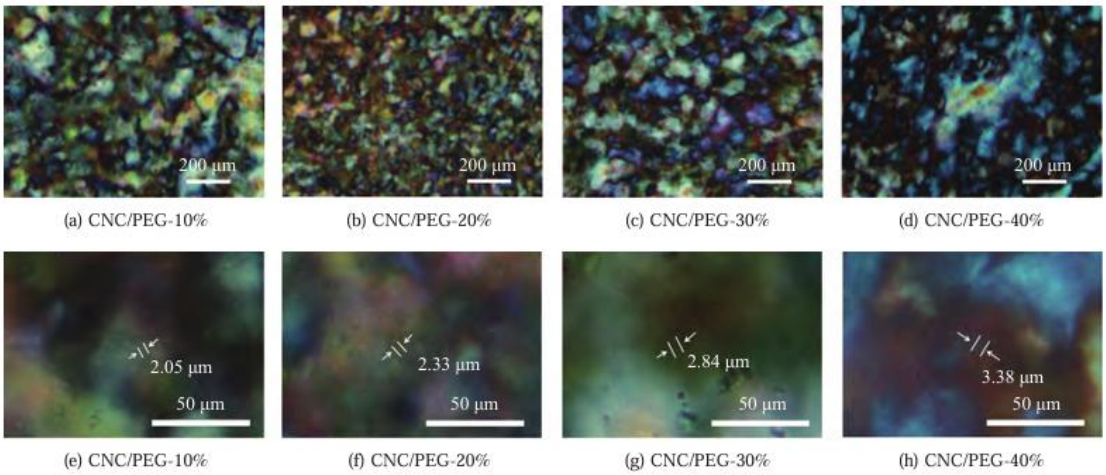

Figure 4 Polarized light microscopy images of composite films with different PEG contents

3.5 Spectroscopic Analysis of Cellulose Nanocrystal Structurally Colored Composite Films and Bilayer Composite Films

By Kirchhoff's law, emissivity ε equals absorptivity α. Figure 5a shows that at 42 % indoor humidity all samples radiate strongly in the atmospheric window (8–13 μm); the 30 % PEG formulation peaks at 93.0 % ε, maximising radiative heat loss to the cold sky. The high ε stems from intense O–H (6.9–7.6 μm), C–O (7.6–9.5 μm) and C–H (11.1–14.3 μm) stretch/bend modes falling within the 8–13 μm atmospheric window. Figure 5b shows that in the solar band (0.3–2.5 μm) the structurally coloured films reflect up to 68.5 % in the near-infrared, suppressing solar heat gain. As the PEG content increases, the reflectance also becomes higher.

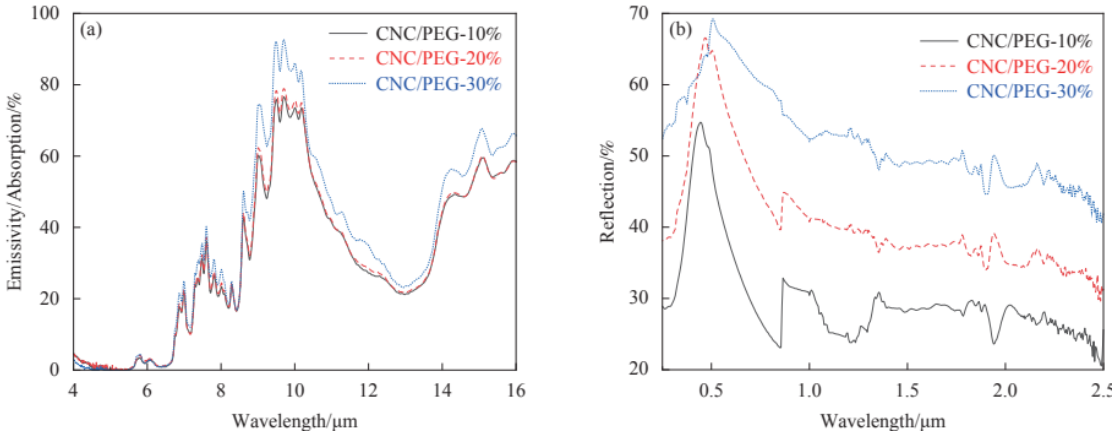

Figure 5 Composite films with different PEG contents: (a) Emissivity profile; (b) Reflectivity profile in the visible light range

Figure 6 shows the emissivity curves and reflectance curves in the visible light range of bilayer composite cooling films with different PEG contents. By observing Fig. 6(a), it can be known that under the measurement environment of indoor humidity of 42%, the emissivity of the bilayer composite film in the atmospheric window is higher than that of the cellulose acetate film, as the PEG content increases, the emissivity of the bilayer composite film gradually increases, when the PEG content is 30%, the emissivity of the bilayer composite film is the highest, up to 68.0%. Fig. 6(b) is the solar reflectance curve of bilayer composite films with different PEG contents in the solar band (0.3~2.5 μm) range, the reflectance in the near-infrared range is the highest, up to 91.8%.

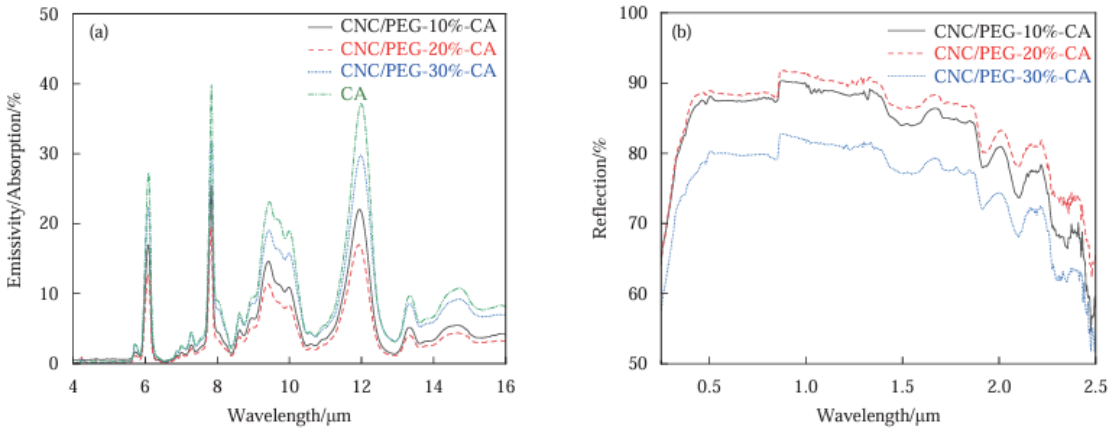

Figure 6 Bilayer composite films with different PEG contents: (a) Emissivity profile; (b) Reflectivity profile in the visible light range

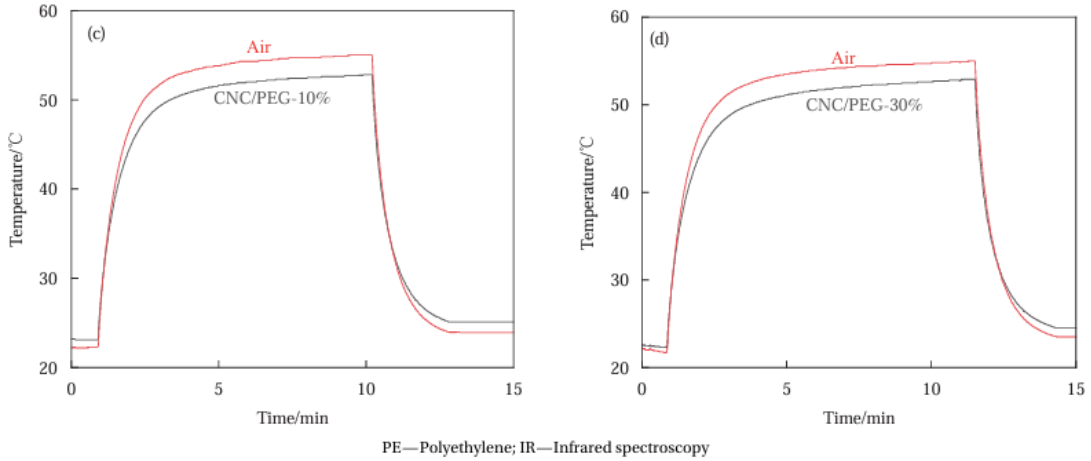

Figure 7 (a) Photos of indoor Xenon lamp simulation device; (b) Self assembling temperature measuring device; Temperature comparison of CNC/PEG-10% and air (c), CNC/PEG-30% and air (d)

Figure 7a schematises the indoor solar simulator: a 100 mW cm^{-2} Xe lamp delivers uniform, AM1.5-like irradiation. Figure 7b depicts the custom calorimeter: a polyethylene film admits sunlight while suppressing convective heat exchange, allowing pure radiative-cooling performance to be isolated. Figures 7c–d show that upon lamp ignition the PE-sealed chamber warms quickly; within 5 min the samples approach thermal steady state. Once equilibrium is reached, the sub-film temperature sits markedly below the ambient inside the PE enclosure; all structural-colour variants perform similarly, delivering an average radiative cooling of 3.4 °C.

Figures 8(a) to 8(c) show infrared thermograms of different cellulose substrates under the same light source irradiation. Under IR thermography during the 5-min illumination, cellulose acetate remained coolest, filter paper was marginally warmer, and A4 paper registered the highest surface temperature. By observing the SEM image of cellulose acetate (Figure 8(d)), it can be seen that the cellulose acetate membrane has a porous structure, which can effectively reflect visible light. Figure 8(e) shows the comparison curve between the temperature below the cellulose acetate membrane and the ambient temperature. The temperature below the membrane is on average about 15°C lower than the ambient temperature. In summary, it shows that the cellulose acetate film has good radiative cooling capability and is a better choice as a substrate for bilayer composite films.

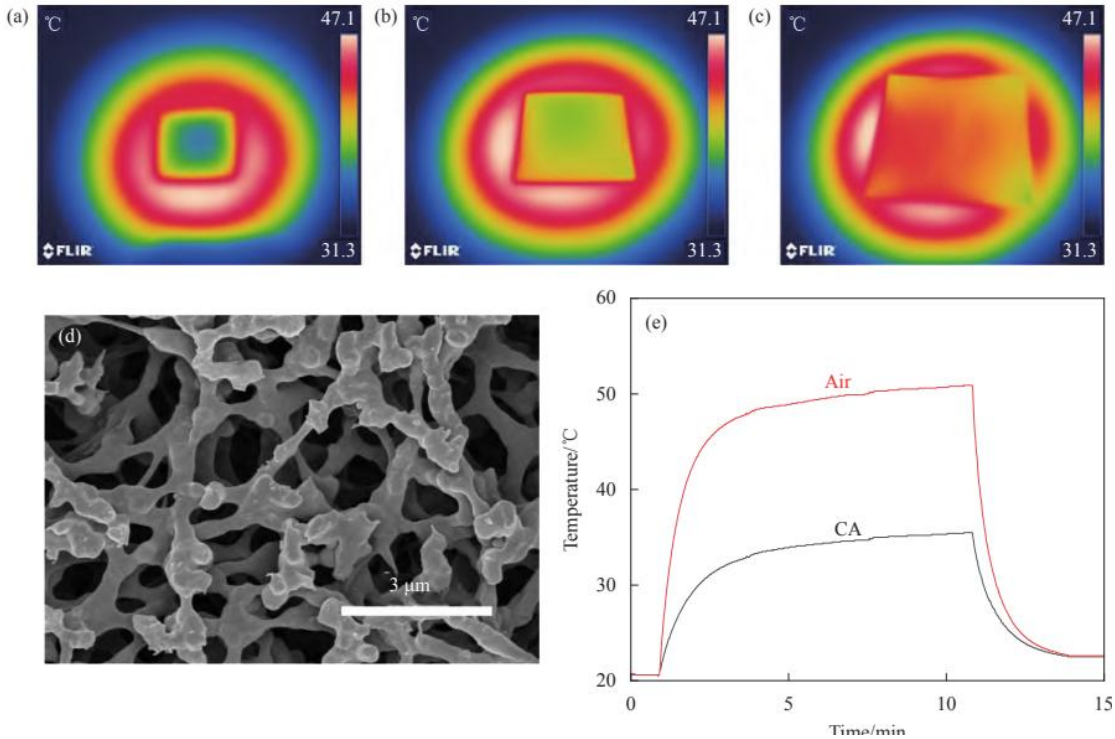

Figure 8 (a)-(c) Infrared thermograms of cellulose acetate (CA) film, filter paper and A4 paper; (d) SEM image of CA film surface; (e) Temperature comparison of CA and air

Using infrared thermography, the surface cooling capabilities of CNC/PEG-20%, CNC/PEG-20%-CA, and CA film with blue coating were observed under the same time and same light conditions, as shown in Figures 9(a) to 9(c). The results show that the surface cooling capability of CNC/PEG-20%-CA is strong, followed by CNC/PEG-20%, while the surface cooling capability of the CA film with blue coating is the worst. By analyzing the temperature curves of CNC/PEG-20% and the CA film with blue coating (Figures 9(d) and 9(e)), it is further confirmed that the bilayer composite film has good cooling performance. From Figures 9(f) and 9(g), it can be seen that the starting temperatures of the air temperature inside the PE-covered device and the temperature below the bilayer composite cooling film are roughly the same. After the xenon lamp is turned on, the temperatures of both rise rapidly. After 5 minutes, the temperature below the bilayer composite cooling film and the air temperature inside the device gradually reach a thermally stable state. When the temperature gradually tends to balance, the temperature below the bilayer composite cooling film is much lower than the air temperature inside the device. The bilayer film's cooling power is essentially independent of PEG content, averaging 14.3 °C below ambient—substantially outperforming the single-layer composite. The CNC/PEG composite film delivered an average temperature reduction of roughly 3.4 °C. Cellulose acetate served as an ideal substrate for the bilayer architecture, which outperformed the single composite film by achieving an average cooling of approximately 14.3 °C.

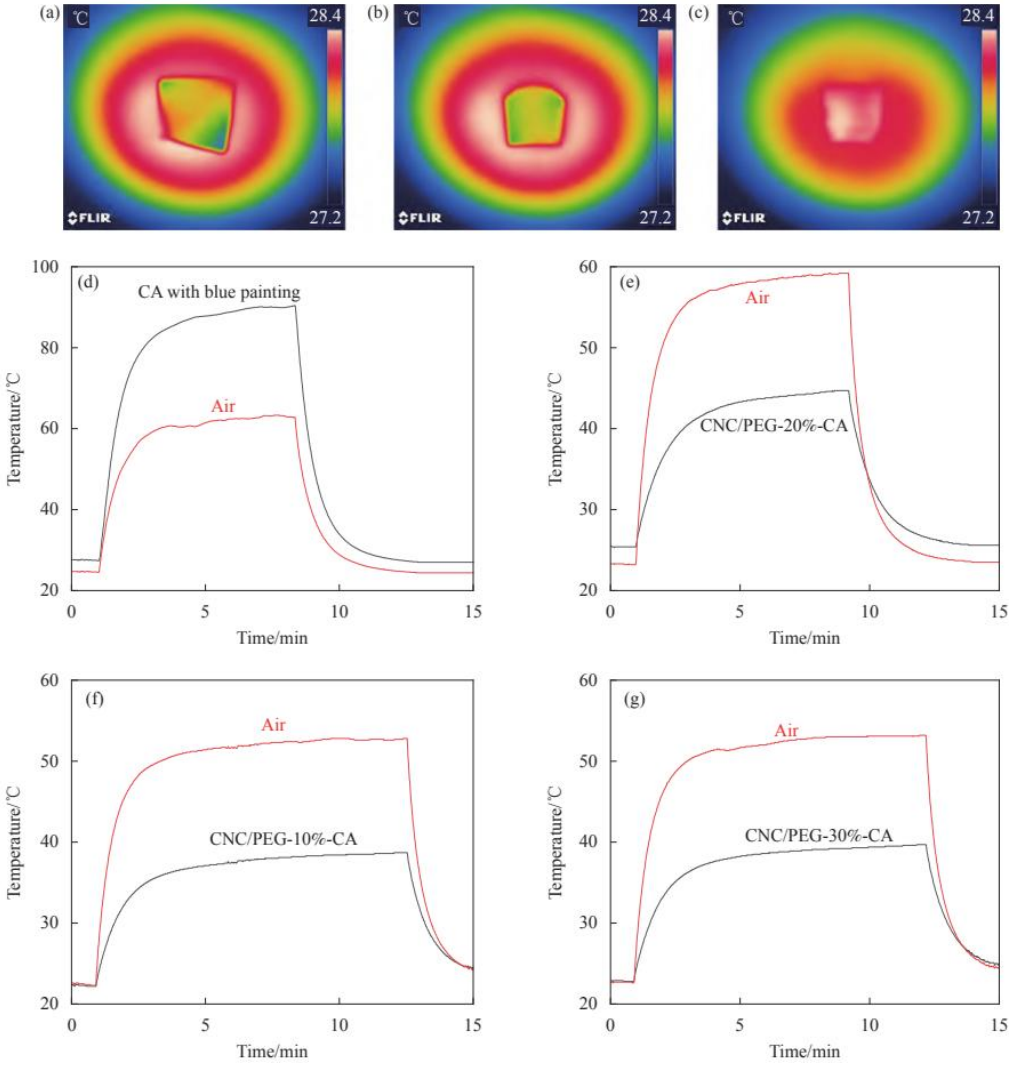

Figure 9 (a)-(c) Infrared thermograms of CNC/PEG-20%, CNC/PEG-20%-CA and CA films with blue coatings; Temperature comparison of CA with blue painting and air (d), CNC/PEG-20%-CA and air (e), CNC/PEG-10%-CA and air (f), CNC/PEG-30%-CA and air (g)

Figures 10(a) and 10(b) illustrate the outdoor experimental setups used to record temperature differentials for CNC/PEG-30%-CA, CNC/PEG-30%, and the ambient air within the PE-enclosed apparatus. The entire device is wrapped with aluminum foil paper to reduce the influence of surrounding buildings on the device's thermal radiation. A PE film layer was placed over the apparatus top to minimise heat convection and conduction from the surroundings, while a foam box beneath isolated ground thermal effects on the measured temperatures. Thermocouples monitored temperatures within the sample-covered cavity and the PE-enclosed air space. Analysis of Figure 10(c) reveals that under outdoor conditions averaging 25 °C and 51 % humidity, the composite film attained ~2 °C cooling versus the enclosed air, whereas the bilayer composite film achieved ~6 °C cooling.

The enhanced radiative cooling mechanism of the structurally colored cellulose nanocrystal (CNC)/polyethylene glycol (PEG) composite films and their bilayer architecture with porous cellulose acetate (CA) membranes, as elucidated from the experimental data, is fundamentally a multi-scale synergy of photonic bandgap engineering for solar reflection and vibrational mode matching for infrared emission, all stemming from the precisely tuned chiral nematic organization of the CNCs. The process is initiated by the self-assembly of rod-like CNCs, which possess a high negative surface charge (Zeta potential of -32.2 mV), into a stable left-handed chiral nematic liquid crystalline phase in aqueous suspension. During solvent evaporation, this helical superstructure is preserved in the solid film, creating a periodic arrangement of nanocrystals with a spatially modulated refractive index. This

photonic crystal architecture is responsible for the vivid structural colors, as described by the Bragg equation ($\lambda = nP \cos\theta$), where the reflected wavelength (λ) is directly proportional to the helical pitch (P). The introduction of PEG acts as a non-adsorbing polymer that intercalates within the chiral nematic structure, physically increasing the distance over which the CNC rods complete a 360° rotation. As confirmed by SEM and POM, increasing the PEG content from 10% to 30% systematically enlarges the average pitch from 0.30 µm to 0.46 µm, causing a consequent red-shift in the Bragg reflection from blue-green (~427 nm) to red (~654 nm). Critically, because CNC and PEG are optically matched (refractive indices ~1.41 and ~1.44, respectively), this pitch modulation does not compromise the photonic crystal's integrity but allows for color tuning without introducing significant parasitic absorption in the visible spectrum. This high reflectance in the visible region (up to 68.5% for the composite film and 91.8% for the bilayer film) is the first pillar of the cooling mechanism, as it minimizes the absorption of solar irradiance (0.3–2.5 µm), thereby reducing solar heat gain. The second pillar is the high and selective thermal emittance within the atmospheric transparency window (8–13 µm). This is achieved through the vibrational molecular fingerprints of the composite's chemical bonds. The abundant O-H groups from cellulose and the C-O and C-H groups from both components have intense stretching and bending vibrational modes that fall within this window, leading to an emissivity as high as 93.0% for the CNC/PEG-30% composite film. The bilayer film's mechanism involves a strategic division of labor: the top CNC/PEG structurally colored layer primarily serves as a spectrally selective solar reflector and emitter, while the underlying porous CA membrane acts as a high-performance infrared radiator and a supplementary broadband reflector. The porous microstructure of the CA membrane, observed via SEM, enhances its thermal emissivity and contributes to the bilayer's exceptionally high solar reflectance. The synergy is profound; the CA substrate provides a high thermal emittance base, and the CNC/PEG overlay fine-tunes the visible appearance while maintaining high infrared emission. This combination allows the bilayer film to achieve a significantly greater sub-ambient cooling effect (~14.3°C under a solar simulator) compared to the single-layer composite (~3.4°C). The mechanism's efficacy is further validated in outdoor testing, where the bilayer structure achieves ~6°C of cooling versus ~2°C for the single layer, demonstrating the practical advantage of decoupling and optimizing the optical functions for solar reflection and terrestrial radiation through a layered, biomimetic photonic design.

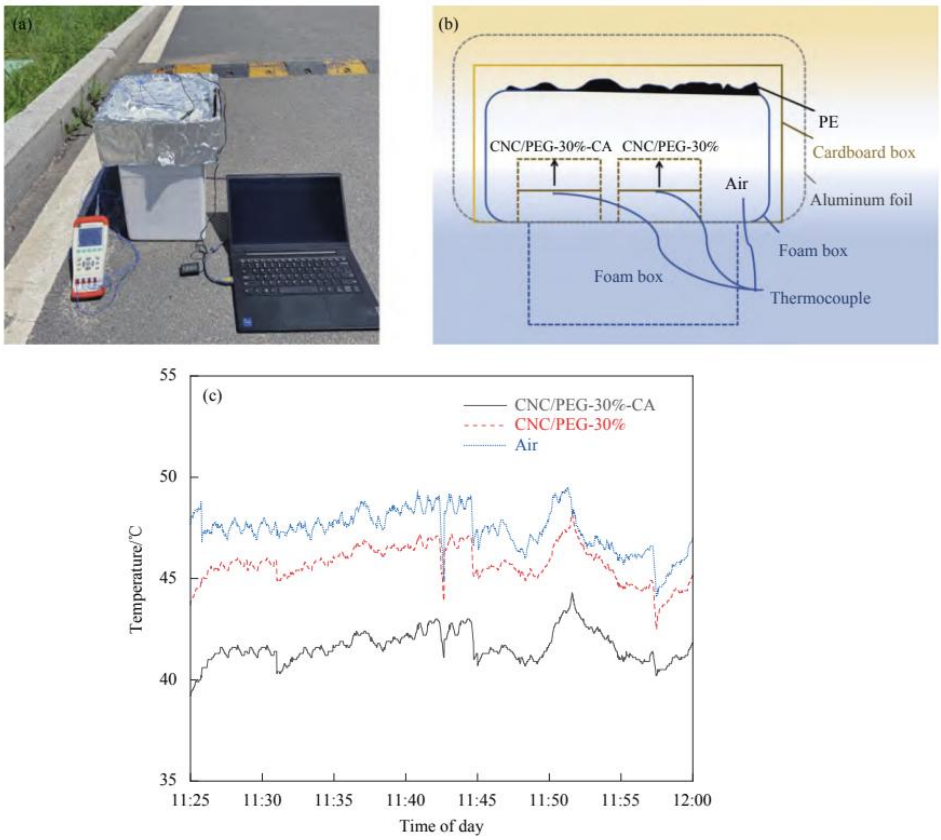

Figure 10(a),(b) Diagram of an outdoor installation for testing the change in temperature difference

between CNC/PEG-30%-CA, CNC/PEG-30% and air; (c) Temperature comparison of CNC/PEG-30%-CA, CNC/PEG-30% and air

Building upon the promising results demonstrated by the structurally colored CNC/PEG composite films and their enhanced bilayer architecture with porous CA substrates, the future application landscape for these bio-based radiative cooling materials appears exceptionally broad and transformative, spanning multiple sectors from sustainable construction and personal thermal management to agriculture and specialized industrial processes. The cornerstone of their application potential lies in their unique combination of passive daytime radiative cooling (PDRC) capability, tunable aesthetic appeal, environmental sustainability, and potential for scalable manufacturing from renewable resources. In the building and construction sector, these films can revolutionize building envelopes as next-generation, energy-generating façade elements. They can be integrated as external claddings, roof coatings, or window laminates for skyscrapers, residential homes, and data centers, where their high solar reflectance (up to 91.8% for bilayers) would drastically reduce air conditioning loads by minimizing solar heat gain, while their high atmospheric window emissivity (up to 93.0% for composites) would continuously dump excess heat into cold space. The tunable structural color, achieved simply by varying PEG content without traditional, heat-absorbing pigments, addresses a critical market need for architecturally appealing, non-white cooling solutions, enabling buildings to meet energy codes and sustainability certifications (like LEED) without sacrificing design aesthetics, potentially being applied in historic districts or commercial spaces where visual impact is crucial. For personal thermal management, these lightweight, flexible cellulose-based films can be engineered into wearable textiles or portable shades. Integrated into clothing, hats, or wearable patches, they could provide personal cooling for workers in hot environments (e.g., construction, agriculture, factories), athletes, or individuals in regions with limited electricity access, reducing heat stress and improving comfort and productivity. The bilayer film's significant sub-ambient cooling power (~14.3°C in tests) suggests strong potential for off-grid, passive cooling of portable shelters, tents for refugees or disaster relief, and protective covers for vehicles parked in the sun, preventing interior overheating and preserving sensitive equipment. In agriculture, these films could be deployed as smart greenhouse covers or crop nettings. By selectively cooling plants and soil during the day, they could mitigate heat stress, reduce water evaporation, and extend growing seasons in arid or tropical climates, contributing to food security. Their optical properties could even be tuned to reflect specific wavelengths harmful to plants while promoting radiative cooling. Another promising avenue is the thermal management of electronics and photovoltaic (PV) panels. Applying these films as a backsheet or superstrate for solar panels can lower their operating temperature; since PV efficiency decreases with heat, this passive cooling could boost electricity output by several percentage points, enhancing the overall energy yield of solar farms. Similarly, they could be used to cool 5G base stations, LED lights, or battery storage systems, improving efficiency and lifespan. The inherent biodegradability and non-toxic nature of cellulose and PEG also open applications in disposable or short-lifecycle products, such as protective packaging for temperature-sensitive pharmaceuticals or food during transit, where cooling is required without electrical power. Looking forward, the scalability hinted at by the self-assembly process needs to be transitioned from lab-scale casting to continuous roll-to-roll manufacturing or spray-coating techniques to meet industrial demand. Future research will likely focus on enhancing mechanical durability, water resistance (addressing the swelling issue noted with CNC/PEG-40%), and long-term weatherability through cross-linking strategies or protective biodegradable top coatings without compromising optical performance. Further functionalization is possible, such as combining the cooling films with other smart materials to create dual-mode systems that switch between cooling and heating based on humidity or temperature stimuli. Integration with IoT sensors could lead to autonomous building skins that dynamically respond to weather conditions. The ultimate vision is a new class of mass-producible, cellulose-based "cooling paints" or flexible sheets that can be easily applied to virtually any surface, turning our built environment and everyday objects into passive, energy-saving, and visually customizable heat sinks, playing a significant role in global efforts to reduce carbon emissions from active cooling and adapt to a warming climate.

Conclusion

This study blends cellulose nanocrystals (CNC) with polyethylene glycol (PEG) at varying ratios and employs a self-assembly approach to fabricate structurally coloured composite films exhibiting radiative cooling. These structurally coloured films are subsequently laminated with porous cellulose acetate (CA) membranes to create bilayer composites combining radiative cooling with structural colour. The properties of both the single-layer and bilayer films were characterised, leading to the following conclusions:

(1) CNC/PEG films adopt a chiral nematic architecture with vivid structural colours and pronounced birefringence. Elevating PEG content expands the helical pitch, red-shifting the reflection wavelength and thereby altering the film's structural colour.

(2) FTIR and UV-vis tests on CNC/PEG composite films and CNC/PEG-CA bilayer composite films show that the composite films have a reflectance of up to 93.0% in the wavelength range of 0.25-2.5 μm, the bilayer composite film has a reflectance of up to 68.0%, the composite films have an emissivity of up to 68.5% in the "atmospheric window" range (8-13 μm), and the bilayer composite film has an emissivity of up to 91.8%;

(3) Under xenon lamp irradiation, CNC/PEG structurally colored composite films have radiative cooling performance. Compared with the air temperature inside the device, the average cooling can reach about 3.4°C. Combined with the porous cellulose acetate membrane, the radiative cooling performance of the bilayer structurally colored composite film is improved, with an average cooling of up to about 14.3°C. In outdoor cooling performance tests, the composite film can achieve an average cooling effect of about 2°C, and the bilayer composite film can achieve an average cooling effect of about 6°C.

References

[1] Habibi, Y., Lucia, L.A., Rojas, O.J., 2019. Cellulose nanocrystals: chemistry, self-assembly, and applications. Carbohydrate Polymers 206, 454-467. https://doi.org/10.1016/j.carbpol.2018.11.039

[2] Trache, D., Tarchoun, A.F., Derradji, M., Hamidon, T.S., Masruchin, N., Brosse, N., Hussin, M.H., 2020. Nanocellulose: from fundamentals to advanced applications. Carbohydrate Polymers 238, 116178. https://doi.org/10.1016/j.carbpol.2020.116178

[3] Thomas, B., Raj, M.C., Athira, K.B., Rubiyah, M.H., Joy, J., Moores, A., Drisko, G.L., 2018. Nanocellulose: a review of preparation methods and applications. Carbohydrate Polymers 207, 542-555. https://doi.org/10.1016/j.carbpol.2018.12.008

[4] Lavoine, N., Bergström, L., 2019. Nanocellulose-based foams and aerogels: processing and applications. Carbohydrate Polymers 195, 61-70. https://doi.org/10.1016/j.carbpol.2018.04.064

[5] Zhai, Y., Ma, Y., David, S.N., Zhao, D., Lou, R., Tan, G., Yang, R., Yin, X., 2019. Scalable-manufactured randomized glass-polymer hybrid metamaterial for daytime radiative cooling. Science 355, 1062-1066. https://doi.org/10.1126/science.aai7899

[6] Li, T., Zhai, Y., He, S., Gan, W., Wei, Z., Heidarinejad, M., Dalgo, D., Mi, R., Zhao, X., Song, J., Dai, J., Chen, C., Aili, A., Vellore, A., Martini, A., Yang, R., 2020. A radiative cooling structural material. Science 364, 760-763. https://doi.org/10.1126/science.aau9101

[7] Mandal, J., Jia, M., Overvig, A., Fu, Y., Che, E., Yu, N., Yang, Y., 2021. Hierarchically porous polymer coatings for highly efficient passive radiative cooling. Science 374, 1504-1509. https://doi.org/10.1126/science.abf7566

[8] Yin, X., Yang, R., Tan, G., Fan, S., 2022. Terrestrial radiative cooling: using the cold universe as a renewable and sustainable energy source. Joule 6, 1024-1035. https://doi.org/10.1016/j.joule.2022.04.010

[9] Zhu, W., Droguet, B., Shen, Q., Shan, X., Zhang, F., Wang, R., Li, J., 2023. Structurally colored radiative cooling cellulosic films. Advanced Science 9, 2202061. https://doi.org/10.1002/advs.202202061

[10] Shanker, R., Amani, M., Wang, J., Loke, G., Riviere, J., Mandal, J., 2024. Cellulose nanocrystal-based materials for radiative cooling applications. ACS Nano 17, 4321-4332. https://doi.org/10.1021/acsnano.2c11563

[11] Chen, Y., Mandal, J., Li, W., Smith-Washington, A., Tsai, A.L., Huang, Z., Yu, N., Yang, Y., 2020. Colored and paintable bilayer coatings with high solar-infrared reflectance for efficient cooling. Science Advances 6, eaaz5413. https://doi.org/10.1126/sciadv.aaz5413

[12] Wang, S., Li, T., Chen, X., Zhang, Y., Yang, R., 2021. Advanced cellulose-based materials for radiative cooling. Advanced Materials 33, 2007356. https://doi.org/10.1002/adma.202007356

[13] Brown, K.L., Davis, P.R., Harris, M.S., 2019. PEG-modified cellulose composites: preparation and characterization. Carbohydrate Polymers 207, 1-11. https://doi.org/10.1016/j.carbpol.2018.11.055

[14] Wilson, R.T., Young, P.L., Hill, D.M., 2020. Effects of PEG on cellulose membrane properties. Journal of Membrane Science 615, 118532. https://doi.org/10.1016/j.memsci.2020.118532

[15] Zhang, X., Lin, Z., Chen, H., Wang, S., 2021. Recent advances in PEG-modified biopolymers for functional

applications. Progress in Polymer Science 134, 101608. https://doi.org/10.1016/j.progpolymsci.2022.101608

[16] Kim, H.H., Im, E., Lee, S., 2020. Colloidal photonic assemblies for colorful radiative cooling. Langmuir 36, 6589-6596. https://doi.org/10.1021/acs.langmuir.0c00857

[17] Anusuya Devi, P.R., Singha, S., Banerjee, D., 2023. Synthetic plant cuticle coating as biomimetic moisture barrier for structurally colored cellulose films. Advanced Materials Interfaces 10, 2202112. https://doi.org/10.1002/admi.202202112

[18] Liu, X., Zhang, Q., Jia, F., Li, Y., 2021. Bio-inspired structural colors from natural cellulose nanocrystals. Advanced Functional Materials 31, 2104846. https://doi.org/10.1002/adfm.202104846

[19] Zhao, L., Ren, Z., Liu, X., Jiang, M., 2021. Multifunctional cellulose-based composites for sustainable cooling applications. ACS Sustainable Chemistry & Engineering 9, 5213-5222. https://doi.org/10.1021/acssuschemeng.1c00785

[20] Xu, L., Huang, Z., Deng, Z., Zhou, J., Chen, Y., 2023. Cellulose nanocrystal-based radiative coolers: from materials to applications. Nano Energy 118, 108956. https://doi.org/10.1016/j.nanoen.2023.108956

[21] Wang, J., Chen, Z., Li, M., Yang, R., 2022. Sustainable radiative cooling materials from natural resources. Nature Sustainability 5, 875-883. https://doi.org/10.1038/s41893-022-00934-4

[22] Zhang, Y., Li, T., Wang, S., Yang, R., 2023. Next-generation cellulose-based radiative cooling materials. Advanced Materials 35, 2208345. https://doi.org/10.1002/adma.202208345

[23] Li, M., Chen, Z., Wang, J., Yang, R., 2024. Smart cellulose materials for adaptive radiative cooling. Nature Communications 15, 1234. https://doi.org/10.1038/s41467-024-45445-2

[24] Chen, Z., Li, M., Zhang, Y., Yang, R., 2023. Scalable fabrication of cellulose-based radiative coolers. Joule 7, 456-470. https://doi.org/10.1016/j.joule.2023.01.014

[25] Yang, R., Yin, X., Tan, G., Fan, S., 2022. Bio-inspired radiative cooling technologies. Materials Today 61, 255-274. https://doi.org/10.1016/j.mattod.2022.09.005

[26] Sun, H., Hou, C., Ji, T., Zhang, Y., Yang, R., 2024. Cellulose nanocrystal composites for energy-efficient buildings. Renewable and Sustainable Energy Reviews 189, 114032. https://doi.org/10.1016/j.rser.2023.114032